Pergamon

PII: S0277-5387(96)00549-9

Polyhedron Vol. 16, No. 18, pp. 3129–3136, 1997

0277-5387/97 $17.00+0.00

π-Complexes of metalloporphyrins as model intermediates in hydrodemetallation (HDM) catalysis

Karen K. Dailey and Thomas B. Rauchfuss*

School of Chemical Sciences, University of Illinois at Urbana-Champaign, Urbana, IL 61801, U.S.A.

Abstract—Transition metal porphyrinate complexes, especially those of nickel and vanadium, are removed from heavy petroleum fractions *via* hydrodemetallation catalysis (HDM). It has been proposed that HDM of metalloporphyrins proceeds *via* the partial hydrogenation of the porphyrin followed by demetallation. It is likely that the hydrogenation of the metalloporphyrin proceeds *via* its complexation to a metal center which transfers hydrogen to the porphyrin. In this paper we discuss recent efforts to simulate this important step. In this study we employ Zn(OEP) (OEP = dianion of octaethylporphyrin) as a model porphyrinate and (arene)Ru^{2+} in the role of an HDM catalyst site. The olive green salt [(cymene)Ru{Zn(OEP)OTf}]OTf (**1**) was characterized by optical and ^1H and ^{13}C NMR spectroscopy, both of which indicate that the cation has C_S symmetry. A crystallographic study shows that the Ru center is π-bonded to one of the four pyrrolide rings, leading to an elongation of one Zn—N bond. It appears that **1** is similar to zinc complexes of *N*-methylporphyrins. Treatment of **1** with HOTf results affords H_4OEP^{2+} *via* the intermediacy of a species $[(cymene)Ru(H_xOEP)]^{n+}$. We also prepared the new complex {(C_5Me_5)Ir[Zn(OEP)OTf]}OTf (**2**) which is fully analogous to **1**. © 1997 Elsevier Science Ltd

Keywords: metalloporphyrins; hydrodemetallation; hydrotreating; petroleum; petroporphyrins; fossil fuels.

Hydrotreating catalysis has been the subject of much research over the past several years, from both the engineering and chemical perspectives [1]. Organometallic studies on this topic have mainly focused on the activation of sulfur and nitrogen heterocycles. In this report we describe some of our studies on a process that is of interest in the beneficiation of fossil fuels, hydrodemetallation, also known as hydrodemetallization (HDM). Since HDM is less frequently discussed by inorganic chemists, we begin this report by summarizing salient aspects of the problem and the associated technologies.

In the United States, the conventional crude petroleum reserves, i.e. those which are relatively inexpensive to acquire and process, were depleted by 21.3% between 1978 and 1991 [2]. This decrease in domestic oil reserves is partially responsible for encouraging an interest in "bottom-of-the-barrel" crude oils [3]. Relative to more volatile components, heavier fractions contain higher concentrations of nitrogen, sulfur, and metals, all of which are undesirable. For volatile fractions obtained by distillation of the crude, the level of contamination by heteroatoms, especially by metals, is often tolerably low. The problem with the heavier fractions is that they require greater processing, since the contaminating heteroatoms damage downstream catalysts. Sulfur and nitrogen are removed from petroleum feedstocks by hydroconversion to H_2S (hydrodesulfurization) and NH_3 (hydrodenitrification) typically using sulfided Co—Mo/Al_2O_3 catalysts. The catalysts utilized in HDS and HDN processes [1,4,5] are susceptible to deactivation by organometallic species thus necessitating that HDM be implemented early in the hydroprocessing sequence.

Metals in petroleum

Crude oils have been shown to contain many different metals. In one survey of 23 U.S. crude oils, 27 elements were detected in residual ash: U, Zn, Zr, V, Sr, Sn, Pb, Ni, Mo, La, Ga, Cu, Ca, Cr, Co, Ce,

*Author to whom correspondence should be addressed.

Ba, B, As, Ag, K, Na, Mg, Mn, Tl, Fe, and Al [6]. The most abundant metals in petroleum are vanadium and nickel, whose combined concentrations sometimes even exceed 1500 ppm [7]. The vanadium content is typically higher than that of nickel.

Vanadium and nickel often occur in petroleum as their porphyrinate complexes. Due to thermal degradation after sediment deposition (diagnesis), the porphyrins found in petroleum differ from their biological precursors especially in terms of their peripheral substituents. The degradation gives rise to a family of petroporphyrins, so called to distinguish them from porphyrins found in living organisms.

The history of petroporphyrins begins with Alfred Treibs who isolated the first petroporphyrin from petroleum sources over 60 years ago [8]. The species Treibs had isolated was vanadyl deoxophylloerythroetioporphyrin, VO(DPEP) [9], as was later established by independent synthesis [10] and crystal structure determination [11]. Treibs realized that these pigments provided definitive proof that petroleum is derived from biological remains. Prior to his work, it had been assumed that petroleum is of inorganic origin, e.g. formed *via* the hydrolysis of metal carbides to give acetylene followed by further transformations. Treibs postulated that chemical and physical changes occurring in sediments result in the conversion of chlorophyll-*a*, the most abundant pigment found in green plants, to the metalloporphyrins of the DPEP series found in petroleum [12,13]. Some years after the identification of VO(DPEP), a second petroporphyrin, nickel etioporphyrin III, was isolated by Glebovskaia and Vol'kenshtein [14] (Scheme 1).

Since petroporphyrins are derived from magnesium complexes, it is at first curious that Mg is virtually absent in the petroporphyrins. The reason for this situation may be found in the relative stabilities of metalloporphyrins, as can be estimated by the acid strength required for their demetallation [15,16]. The acid stability of metalloporphyrins in general correlates inversely with the electronegativity of the metal. Porphyrinates of electropositive metals, e.g. Mg^{2+} and Zn^{2+}, display enhanced basicity at the pyrrolic nitrogen, facilitating protonation at nitrogen leading to decomplexation. Conversely, the more electronegative metal centers, such as Ni^{2+} and VO^{2+}, form acid-stable porphyrinates.

Hydrodemetallation in petroleum refining

The hydrodemetallation (HDM) of petroleum is of growing industrial importance due in large measure to increased interest in heavier fractions that are contaminated by the metallopetroporphyrins. Thus, HDM is more commonly associated with the processing of the products of fluid catalytic cracking (FCC) and hydrocracking (HCR) as well as vacuum residua (b.p > 500°C). At the outset, it is important to recognize that the species targeted by this process are not petroporphyrins, *per se*, but the metals derived from the porphyrins. These metals are blamed for the formation of oxide and sulfide deposits that passivate the catalysts and corrode the reactors. The macrocyclic petroporphyrins are however important as they serve as the vehicles that solubilize and deliver the poisoning metals to the catalysts used in the refining process.

A number of postulates have been advanced for HDM catalysis [1]. In one theory, the porphyrin π-system interacts with Mo sites inducing demetallation under reducing conditions [17]. It has also been proposed that in the presence of H_2/H_2S (i.e. the reducing conditions in hydrotreatment), porphyrinate metal–sulfur interactions weaken the metal–nitrogen bonds of the metalloporphyrin leading to eventual demetallation [18]. Wei and coworkers [19] proposed that HDM proceeds *via* partial hydrogenation of the metalloporphyrin to give metallochlorins and metallobacteriochlorins [20,21].

Models for metal–metalloporphyrin interactions

Regardless of the mechanism(s) of HDM, an early step in the process is very likely to involve the inter-

Scheme 1

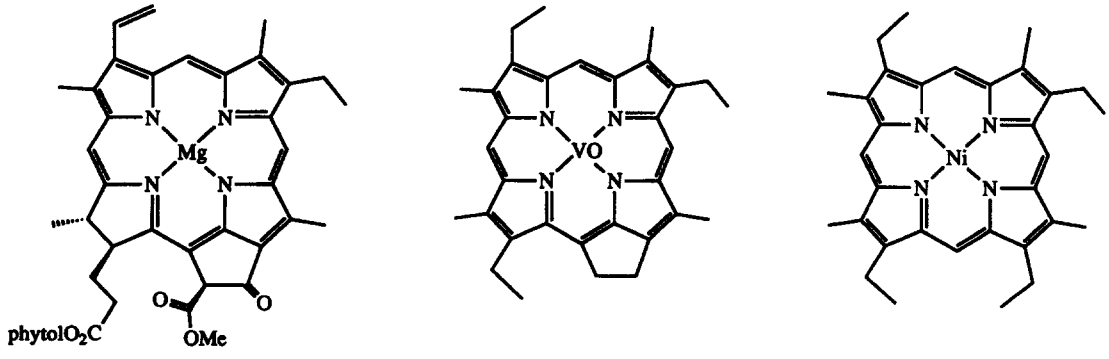

Chlorophyll-a VO(DPEP) Ni(etioporphyrin III)

Scheme 1.

action of a metalloporphyrin with a second metal center. It is thus relevant to mention that numerous bimetallic metalloporphyrins are known, although invariably the two metals interact with the porphyrin exclusively *via* the pyrrolide nitrogen atoms. Metal coordination to the periphery of metalloporphyrins has not, however, been observed prior to our work.

In our first study in this area we showed that treatment of Ni(OEP) with sources of (cymene)Ru^{2+} results in the formation of $\{(cymene)Ru[\eta^5\text{-}Ni(OEP)]\}^{2+}$ (cymene is 4-isopropyltoluene) [22]. This adduct was characterized by a number of spectroscopic methods as well as a single crystal X-ray diffraction study of the BF_4^- salt (eq. (1)).

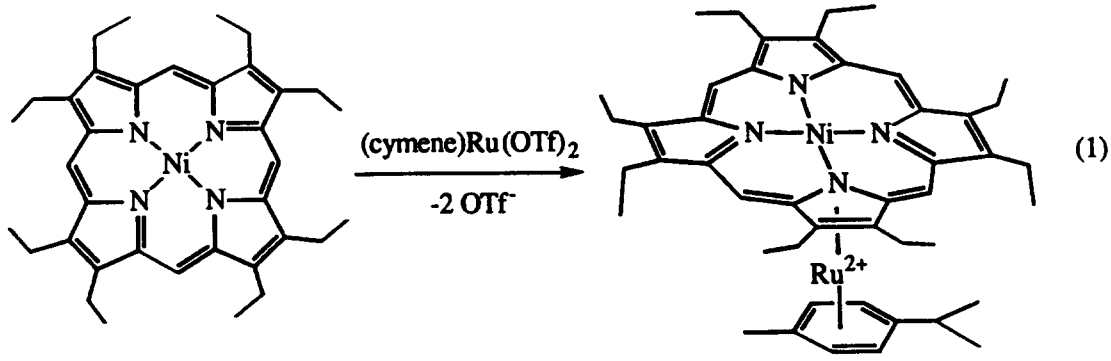

(1)

The crystallographic analysis showed that the Ni(OEP) ligand is strongly distorted upon π-complexation. For example, the three uncomplexed pyrrolide rings are twisted 10°, 28°, and 27°, respectively, from the least-squares plane of the Ru-bound pyrrolide giving rise to a ruffled conformation of the metalloporphyrinate.

The present work extends the studies on nickel complexes focusing on the use of Zn(OEP), which has the advantage of binding more strongly to ruthenium than does Ni(OEP). The Ru—Zn(OEP) complex crystallizes very well, which has allowed us to conduct a crystallographic analysis that is of higher quality than the previously reported Ni—Ru species. We have discovered that these zinc complexes are five coordinate which has prompted us to propose an analogy between the new class of σ,π-dimetallated porphyrins and the complexes of *N*-methylporphyrins.

RESULTS

Treatment of an orange CH_2Cl_2 solution of (cymene)$Ru(OTf)_2$ with a magenta solution of Zn(OEP) resulted in the formation of an olive green product. The mixture was refluxed at 65°C to compensate for the low solubility of Zn(OEP) in CH_2Cl_2. Upon addition of Et_2O the product precipitated from the reaction solution and unreacted Zn(OEP) was removed by washing with Et_2O. Microcrystals of $\{(cymene)Ru[Zn(OEP)OTf]\}(OTf)$ (**1**) were obtained in 67% yield (eq. 2).

$$(cymene)Ru(OTf)_2 + Zn(OEP) \longrightarrow \underset{(1)}{\{(cymene)Ru[Zn(OEP)OTf]\}(OTf)} \quad (2)$$

Complex **1** is air stable and readily soluble in polar organic solvents. Solutions of **1** decompose in coordinating solvents such as DMF and MeCN, although this process is not as fast as with $\{(cymene)Ru[Ni(OEP)]\}^{2+}$ [22].

The UV-visible spectrum of **1** (Fig. 1) is consistent with a decreased symmetry for the coordinated Zn(OEP) moiety. The Soret band of **1** is broadened and is shifted to 412 nm *vs* the sharp transition at 394 nm in the spectrum of Zn(OEP). As for the Ni(OEP) adduct, the optical spectrum shows a transition at 754 nm, which is not observed in free Zn(OEP). The ^1H NMR spectrum of **1** confirms the lower symmetry of **1** compared to that of Zn(OEP). Two methyne signals are observed (δ 8.05 and 7.89), consistent with C_S symmetry. These signals are shifted upfield from the methyne resonance at δ 10.21 in free Zn(OEP), indicating that complexation reduces the ring current

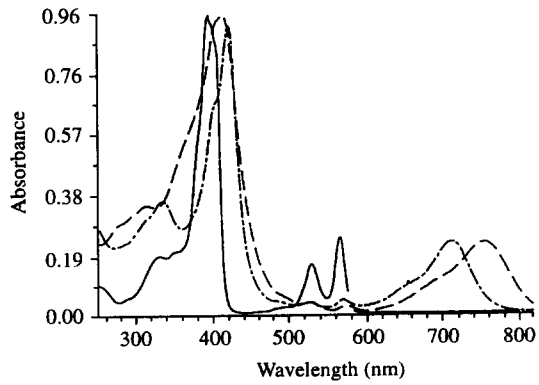

Fig. 1. UV-vis spectra (CH_2Cl_2 solns) for Zn(OEP) (solid), $\{(cymene)Ru[Zn(OEP)OTf]\}OTf$ (– – –), and $\{(C_5Me_5)Ir[Zn(OEP)OTf]\}(OTf)$ (– · – · –).

of the metalloporphyrin. The rich set of methylene resonances is also consistent with the proposed structure. The ^{13}C NMR spectrum shows 25 resonances, as predicted.

The IR spectrum of **1** is more complicated than originally expected. In addition to the characteristic $\nu_{S=O}$ at 1268 (asym) and 1031 (sym) cm^{-1} for the free $CF_3SO_3^-$, there are bands which we assign to $\nu_{S=O}$ for coordinated $CF_3SO_3^-$, i.e. 1316, 1211 (asym), and 957 (sym) cm^{-1}. The bands for the triflate ligand are analogous to those found in covalent triflate derivatives such as organic triflate esters [23] and covalent inorganic derivatives, e.g. $(Bu_4N)_2[Mo_6Cl_8(CF_3SO_3)_6]$ [24]. On the basis of these data, it appears that one $CF_3SO_3^-$ group in **1** is coordinated to Zn^{2+}. The square pyramidal coordination sphere is typical of zinc porphyrinates although it is unexpected that the fifth ligand would be the poorly basic triflate anion.

The $(C_5Me_5)Ir^{2+}$ adduct, {(C_5Me_5)Ir[Zn(OEP)OTf]}OTf (**2**), was prepared in 64% yield following the procedure used to synthesize **1**. Compound **2** is spectroscopically very similar to **1**. For example, its IR spectrum also indicates two $CF_3SO_3^-$ environments.

Solid state structure of **1**

A single crystal X-ray diffraction study on **1** confirmed that the (cymene)Ru^{2+} moiety is π-bound to a pyrrolide of the Zn(OEP) (Fig. 2) [25]. It can also be seen that the Zn^{2+} is pentacoordinate with an N_4O coordination sphere. The pyrrolide and arene planes deviate from parallel by only 1.90° (Table 1). The Zn^{II} atom is displaced 0.378 Å from the plane of the four pyrrolide nitrogen atoms. This displacement of the Zn is somewhat greater than in Zn(OEP)py (0.31 Å) [26] and Zn(OEP)(MeIm) (0.35 Å) [27]. This difference may reflect the competition between Zn^{2+} and Ru^{2+} for electron density at N. The Ru—N1 distance in **1** is only 0.034 Å longer than that of [(cymene)Ru(η^5-C_4Me_4N)]$(OTf)_2$ [22]. More interestingly, the Zn—N1 distance of 2.161 Å is much longer than the Ni—N distance of 1.963 Å in {(cymene)Ru[Ni(OEP)]}$^{2+}$. The average Zn—N (pyrrolide) distances in the aforementioned pyridine and methylimidazole adducts are 2.067 and 2.068 Å, respectively.

Protonolysis of {*(cymene)Ru[Zn(OEP)OTf]*}$^+$

Treatment of a CH_2Cl_2 solution of {(cymene)Ru[Zn(OEP)OTf]}OTf with 10 equiv. of HOTf resulted not only in the demetallation of the Zn(OEP), but also destroyed the Ru-pyrrolide bonding. ^1H NMR analysis of the reaction mixture showed the formation of $H_4(OEP)^{2+}$, indicated by its distinctive methyne resonance at δ 10.64 as well as an equally intense N*H* signal at δ −4.0. Treatment of **1** with 3.5 equiv. of HOTf gave a green (*vs* olive green) solution. Over a period of ~24 hs, this solution assumed a purple color signaling the formation of $H_4(OEP)(OTf)_2$ (Fig. 3). When the protonation was monitored by ^1H NMR spectroscopy, an intermediate could be detected immediately upon addition of the HOTf. This intermediate is characterized by pair of new porphyrin C*H* (meso) resonances at δ 8.88 and 8.22, indicative of C_s symmetry. Over a period of several hours at room temperature, this species develops as the dominant solution species prior to its decomposition to H_4OEP^{2+} (eq. 3).

$$\{\text{(cymene)Ru[Zn(OEP)OTf]}\}^+ \xrightarrow{x\text{H}^+} \underset{\textbf{(1)}}{} \qquad (3)$$

$$[\text{(cymene)Ru(H}_x\text{OEP)}]^{x+} \xrightarrow{(4-x)\text{H}^+} \text{H}_4\text{OEP}^{2+}$$

In one experiment the solvent was evaporated when

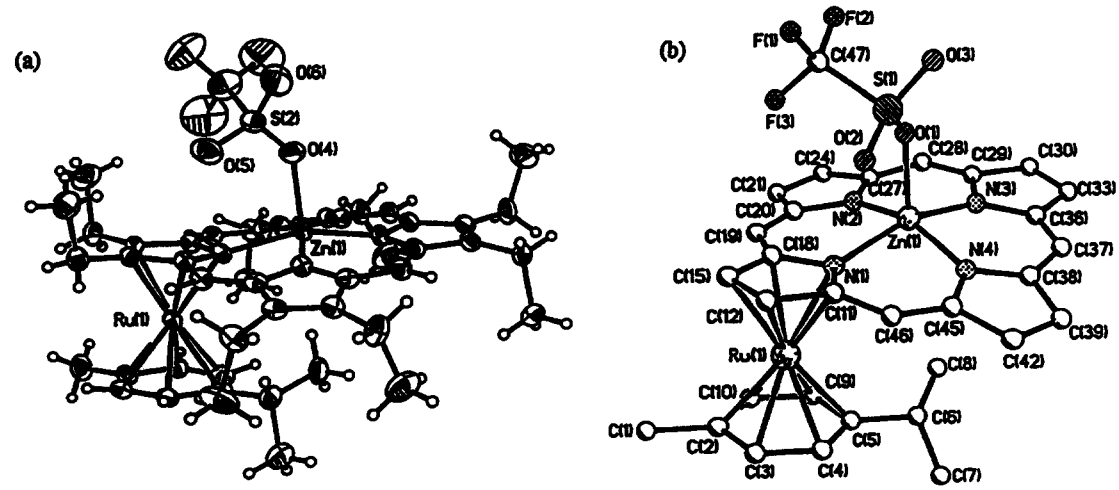

Fig. 2. Two views of the cation in {(cymene)Ru[Zn(OEP)OTf]}(OTf) with thermal ellipsoids drawn at the 50% probability level. Ethyl groups were omitted in the right-hand picture for clarity.

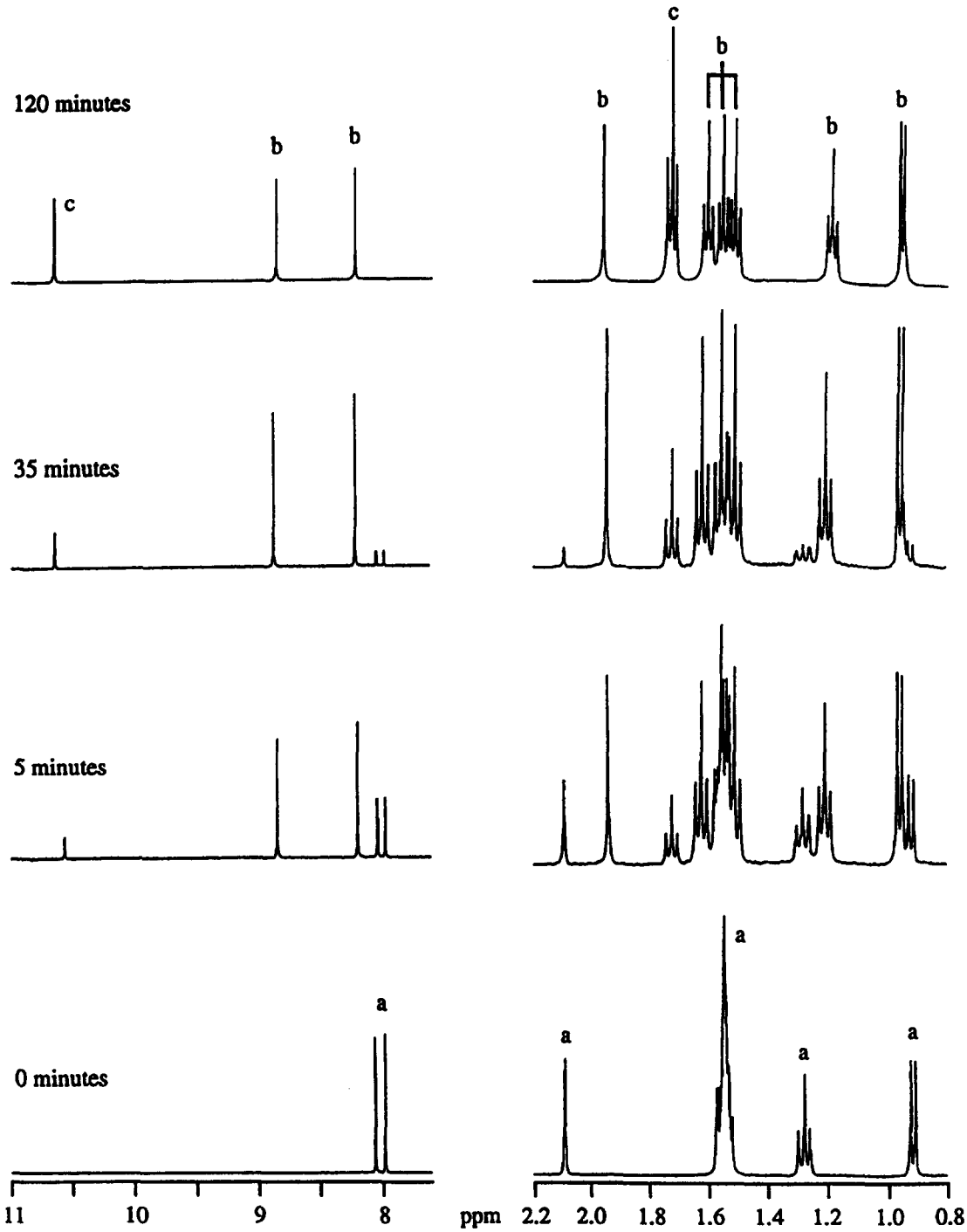

Fig. 3. ^{1}H NMR spectra (CD_2Cl_2, 400 MHz) for stages in the reaction of {(cymene)Ru[Zn(OEP)}OTf]}(OTf) with 3.5 equiv. HOTf at room temperature. Signals are labeled for the starting complex (a), the zinc-free intermediate (b), and H_4OEP^{2+} (c).

the intermediate was at its maximum concentration. Analysis of the residue by fast atom bombardment (FAB) mass spectroscopy revealed a strong peak envelope centered at 770.4 m/z which corresponds to the molecular ion of (cymene)Ru(H_nOEP)$^{2+}$ ($n = 0$ or 1). This peak envelope is not present in FAB mass spectrum of **1**. These preliminary findings suggest that it will be possible to isolate and fully characterize the zinc-free complex. It should be noted, however, that in contrast to the behavior of **1**, {(cymene)Ru-[Ni(OEP)]}$^{2+}$ is relatively unreactive towards HOTf.

DISCUSSION

The role of metalloporphyrins as ligands is closely related to the coordination chemistry of pyrroles and pyrrolides [28]. Pyrrolides are commonly observed as σ-bonded amido-like ligands but there are also many examples of π-complexes with η^5-pyrroles [29] and η^5-pyrrolides ($NC_4R_4^-$) ligands [30]. η^2- and η^4-pyrrolides [31,32] have also been observed as ligands, although they are less common. More relevant to the new coordination mode, pyrrolides can bind simultaneously in both η^1- and η^5-modes (Scheme 2) [33].

Based on this background, the ability of metalloporphyrins to serve as π-ligands is not completely surprising.

Complexes **1** and **2** are in many ways similar to complexes of *N*-alkylporphyrins [34], e.g. M(*N*-MeTPP)Cl where M = Zn [35], Co [36], and Mn [37] (TPP = dianion of tetraphenylporphyrin). In both the *N*-methyl and π-complexed porphyrins, a pyrrolide nitrogen atom is bound to two substituents, the central metal atom and the *N*-bonded substituent (CH_3 or Ru). Crystallographic studies of *N*-alkylporphyrinatometal(II) complexes show that the alkylated nitrogen–metal bonds are longer than the nonalkylated nitrogen–metal bonds and that the metals are often five coordinate:

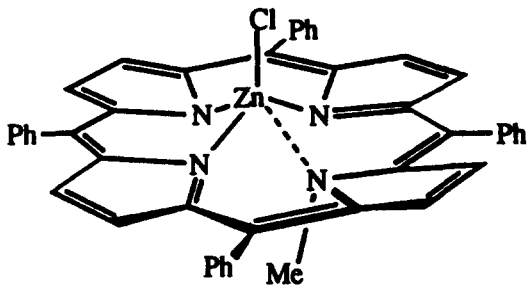

Zn(*N*-MeTPP)Cl

For example in Zn(MeTPP)Cl the Zn—N(Me) distance is 0.5 Å longer than the other three Zn—N bonds. The *N*-alkyl pyrrole ring is also greatly tilted away from the mean plane of the molecule—a consequence of the sp^3-hybridization of the *N*-methyl group. Spectroscopic properties of **1**, **2**, and the metallated *N*-alkylporphyrins are also similar. For example, Zn(*N*-MeOEP)Cl [38] exhibits a Soret band (422 nm) which is red-shifted from that of Zn(OEP) (394 nm). The Soret bands of other *N*-alkylporphyrinato complexes also are either broadened or split [34]. Overall the UV-visible spectra indicate a loss in aromatic character. For example, the appearance of the transitions at 672 and 636 nm for complexes **1** and **2**, respectively, are similar to the strong low energy bands characteristic of metallochlorins [39].

This project was conceived in order to study the interactions of transition metals with metalloporphyrins, a likely early step in HDM catalysis. Coordination of Ru^{II} and Ir^{III} does affect the structures of the metalloporphyrins but does not induce spontaneous demetallation of the Zn(OEP) moiety although the π-complexation does weaken one Zn—N bond. Furthermore it is likely that attachment of the cationic arenophilic metal actually decreases the basicity of the metalloporphyrin, rendering it less susceptible to proton-induced demetallation. It is evident from this and the previous study [22] that the metal in the N_4 core has a profound influence of the π-basicity of the porphyrin: the zinc complex undergoes protonolysis, the nickel complex does not (at least not readily) and we cannot even prepare the vanadium adduct. This series parallels the electropositive character of the central metal. Our work does show that porphyrin hydrogenation could proceed *via* π-complexes similar to **1** and **2**. It will therefore be of interest to explore the hydrogenation of M(OEP) complexes such as **1**.

The use of *metallo*porphyrins for ring transformations of the macrocycle followed by demetallation is an established strategy. For example, octabromotetraphenylporphyrin is prepared by the bromination of Cu(TPP) followed by acid demetallation with perchloric acid [40]. Without the metal center, the bromination is incomplete. Our work suggests that related strategies utilizing Zn(OEP) could be used similarly to give a new family of metalloporphyrin complexes where the metal is not bound to the N_4 core.

EXPERIMENTAL

Syntheses and workups were performed under an inert atmosphere of purified nitrogen unless otherwise

η^1-pyrrolide

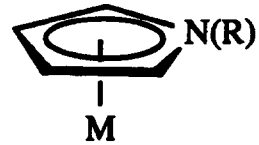

η^5-pyrrolide or η^5-pyrrole

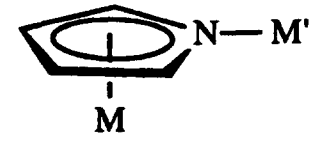

η^1:η^5-pyrrolide

Scheme 2.

stated. Most reagents and solvents were used as received from Aldrich. Literature methods were followed for the preparation of $[(cymene)RuCl_2]_2$ [41], $[(C_5Me_5)IrCl_2]_2$ [42], and Zn(OEP) [43]. Celite 545 was obtained from Fisher Scientific and dried before use. The silica gel (0.040–0.063 mm, 230–400 mesh ASTM) for the chromatographic separations was procured from Merck.

IR spectra were acquired on KBr pellets using a Mattson Galaxy Series FTIR 3000 spectrometer and the data are reported in cm^{-1}. NMR spectra were collected on Varian Unity 400, General Electric GN500, or Varian Unity 500 spectrometers. Fast atom bombardment mass spectra were recorded with a VG ZAB-SE and are reported in units of m/z. UV-visible spectra were obtained on a HP-8452A diode array spectrophotometer.

Preparation of {(cymene)Ru{Zn(OEP)OTf]}OTf, **1**. A 100 cm^3 Schlenk flask was charged with 0.026 g (0.042 mmol) of $[(cymene)RuCl_2]_2$, 0.044 g (0.170 mmol) of AgOTf, and 10 cm^3 of CH_2Cl_2. The slurry was filtered through Celite and the resulting orange solution was treated with 0.075 g (0.125 mmol) of Zn(OEP). The slurry was refluxed at 65°C for *ca* 16 h. After cooling to room temperature, the dark purple solution was filtered (in air) to remove the unreacted

Table 1. Selected bond lengths (Å) and Pyrrolide tilt angles[a] (°) for {(cymene)Ru[Zn(OEP)OTf]}OTf (**1**)

Bond lengths (Å)			Pyrrolide tilt angles (°)		
Zn—N1	2.161(3)	Ru—C12	2.242(4)	N1—N2	13.31
Zn—N2	2.072(3)	Ru—C15	2.241(4)	N1—N3	8.03
Zn—N3	2.021(3)	N1—C11	1.397(5)	N1—N4	14.04
Zn—N4	2.069(3)	N1—C18	1.402(5)	N2—N3	16.97
Ru—N1	2.183(3)	Zn—O1	2.084(3)	N3—N4	6.46
Ru—C11	2.186(4)	Ru—N1	1.848*	N2—N4	23.09
Ru—C18	2.189(4)	Ru—η^6—cymene	1.707*	N1—cymene	1.90

[a]angle formed at the intersection the two respective pyrrolide planes containing either N1, N2, N3, or N4; calculated from least-squares planes.

Table 2. Crystal data and structure refinement details for **1**

Empirical formula	$C_{52}H_{66}F_6N_4O_7RuS_2Zn$
Formula weight	1203.65
Temperature (K)	198(2)
Wavelength (Å)	0.71073
Crystal system, space group	monoclinic, $P2_1/n$
a = 15.3312(2) (Å)	
b = 22.0805(3) (Å)	
c = 16.7185(3) (Å)	
α = 90 (°)	
β = 100.9080(10) (°)	
γ = 90 (°)	
V = 5557.30(14) ($Å^3$)	
Z = 4	
Density (calculated) (Mg/m^3)	1.439
Absorption coefficient (mm^{-1})	0.851
Crystal size (mm)	0.44 × 0.34 × 0.06
Theta range (°)	1.55–28.24
Index ranges	$-18 \leqslant h \leqslant 19$, $-28 \leqslant k \leqslant 27$, $-14 \leqslant l \leqslant 22$
Collection method	CCD area detector frames
Reflections collected	35582 [R (int) = 0.0562]
Independent reflections	13201 [9256 obs, $I > 2\sigma(I)$]
Absorption correction	Integration
Refinement (shift/err = 4.831)	Full-matrix least-squares on F^2
Data/restraints/parameters	13185/0/658
Goodness-of-fit on F^2	1.118
Final R indices (obs. data)	R_1 = 0.0530, wR_2 = 0.0985
R indices (all data)[a]	R_1 = 0.0935, wR_2 = 0.1209
Largest diff. peak and hole ($e^-/Å^3$)	0.521 and −0.542

[a]$w = 1/[\sigma^2(F_0^2) + (0.0109P)^2 + 7.5500P]$, where $P = (F_0^2 + 2F_c^2)/3$.

Zn(OEP). The remaining Zn(OEP) was removed by first precipitating the complex with Et_2O and washing with Et_2O until the filtrate was colorless. Single crystals were obtained by layering a CH_2Cl_2 solution of **1** with hexane. Yield: 0.065 g (67%). ^1H NMR (CD_2Cl_2): δ 8.05 (s, 2H), 7.89 (s, 2H), 5.7 (dd, 4H), 3.44 (m, 2H), 3.30 (m, 14H), 2.43 (m, 1H), 2.09 (s, 3H), 1.54 (m, 18H), 1.29 (m, 6H), 0.92 (d, 6H). $^{13}C\{^1H\}$ NMR (CD_2Cl_2): δ 167.24, 163.80, 155.78, 147.34, 147.11, 145.81, 111.96, 108.78, 104.98, 102.56, 102.07, 96.63, 88.37, 86.10, 31.40, 22.18, 19.02, 18.92, 18.91, 18.70, 18.67, 17.34, 16.90, 16.51, 15.89. FAB-MS: 832.3 (M^+). IR: $\nu_{S=O}$ (anion) = 1268 (asym), 1031 (sym); $\nu_{S=O}$ (ligand) = 1316 and 1211 (asym), 957 (sym); ν_{CF} = 1158 (asym), 1236 (sym); δ(OSO) = 637. UV-vis (CH_2Cl_2), λ [nm] (ε [M^{-1} cm^{-1}]): 274 (22000), 312 (25000), 370 (41000), 412 (65000), 528 (4000), 576 (3500), 692 (8500), 754 (17000). Anal. Found: C, 50.83; H, 5.50; N, 4.39. Calc. for $C_{48}H_{58}N_4F_6O_6RuS_2Zn$: C, 50.95; H, 5.17; N, 4.95.

Preparation of $\{(C_5Me_5)Ir[Zn(OEP)OTf]\}OTf$, **2**. A 100 cm^3 Schlenk flask was charged with 0.033 g (0.042 mmol) of $[(C_5Me_5)IrCl_2]_2$, 0.043 g (0.166 mmol) of AgOTf, and 10 cm^3 of CH_2Cl_2. The slurry was filtered through Celite to remove AgCl. To this solution was added 0.075 g (0.125 mmol) of Zn(OEP). The reaction mixture was refluxed for *ca* 16 h. After cooling to room temperature, the reaction mixture was filtered (in air) to remove the unreacted Zn(OEP). The crude product was reprecipitated from THF solution by the addition of hexane until the supernatant was colorless. A green powder was recovered. Yield: 0.065 g (64%). ^1H NMR (CD_2Cl_2): δ 8.27 (s, 2H), 8.14 (s, 2H), 3.49 (m, 2H), 3.38 (m, 12H), 3.19 (m, 2H), 1.70 (t, 6H), 1.60 (m, 18H), 0.88 (s, 15H). $^{13}C\{^1H\}$ NMR (CD_2Cl_2): δ 166.68, 163.59, 155.65, 148.14, 147.32, 145.83, 108.94, 107.09, 98.87, 95.94, 94.53, 19.14, 19.05, 19.03, 17.85, 17.43, 17.05, 16.83, 15.90, 8.04. FAB-MS: 924.2 (M^+). IR: $\nu_{S=O}$ (anion) = 1280 (asym), 1030 (sym); $\nu_{S=O}$ (ligand) = 1305 and 1215 (asym), 959 (sym); ν_{CF} = 1160 (asym), 1234 (sym); δ(OSO) = 637. UV-vis (CH_2Cl_2), λ [nm] (ε [M^{-1} cm^{-1}]): 334 (29000), 404 (51000), 420 (71000), 526 (4400), 572 (5000), 712 (19000). Anal. Found: C, 47.20; H, 4.97; N, 4.50. Calc. for $C_{48}H_{59}N_4F_6IrO_6S_2Zn$: C, 47.11; H, 4.86; N, 4.58.

Protonolysis of $\{(cymene)Ru[Zn(OEP)OTf]\}^+$. A 100 cm^3 Schlenk flask was charged with 0.030 g (0.027 mmol) of $\{(cymene)Ru[Zn(OEP)OTf]\}OTf$ and 10 cm^3 of CH_2Cl_2 to give an olive green solution. Approximately 0.008 cm^3 (0.093 mmol) of HOTf was added to the mixture by microsyringe. The solution color immediately changed to green. After 5 min, a 1 cm^3 aliquot was removed from the mixture, exposed to air, and taken to dryness under vacuum. Further samples were removed after 35 and 120 min. The following spectroscopic data are given for the sample taken at 120 min. Note that as shown in Fig. 3 these samples contain some $[H_4(OEP)](OTf)_2$. ^1H NMR (CD_2Cl_2): δ 8.88 (s, 2H), 8.22 (s, 2H), 6.03 (d, 2H), 5.93 (d, 2H), 3.60–3.42 (overlapping m, 6H), 3.55 (m, 8H), 3.12 (m, 2H), 2.61 (1H), 1.95 (s, 3H), 1.62 (t, 3H), 1.56 (t, 3H), 1.51 (t, 3H), 1.20 (t, 3H), 0.95 (d, 6H). FAB-MS: 770.4 (M^+). UV-vis (CH_2Cl_2, nm): appearance of band at 718. ^1H NMR (CD_2Cl_2, $[H_4OEP](OTf)_2$): δ 10.61 (s, 4H), 4.17 (q, 16H), 1.72 (t, 24H), −4.0 (s, 4H). FAB-MS: 535.4 ($H_4(OEP)^{2+}$). UV-vis (CH_2Cl_2, $[H_4(OEP)](OTf)_2$, nm): 404, 548, 592.

Crystal data and structure refinement summary for **1**. The data crystal was mounted using oil (Paratone-N, Exxon) to a thin glass fiber. The sample was bound by faces (1 0 −1), (−1 0 1), (0 1 0), (0 −1 0), (1 0 1), and (−1 0 −1). Distances from the crystal center to these facial boundaries were 0.040, 0.040, 0.170, 0.170, 0.22, and 0.22 mm, respectively. Crystal and refinement details are given in Table 1. Systematic conditions suggested the space group $P2_1/n$. Standard intensities monitored during frame collection showed no decay; decay correction was not applied. Intensity data were reduced by 3D-profile analysis using SAINT [44] and corrected for Lorentz-polarization effects and for absorption. Scattering factors and anomalous dispersion terms were taken from standard tables [45].

The structure was solved by direct methods [46], the correct metal atom positions were deduced from a vector map. Subsequent cycles of isotropic least-squares refinements followed by an unweighted difference Fourier synthesis revealed positions for the remaining non-H atoms. Methyl H atom positions were optimized by rotation about C—C bonds with idealized C—H and H—H distances. Remaining H atoms were included as fixed idealized contributors. H atom *U*s were assigned as 1.2, 1.2, and 1.5 times U_{eq} of adjacent C atoms for CH, CH_2 and CH_3 groups, respectively. Non-H atoms were refined with anisotropic thermal coefficients. Successful convergence of the full-matrix least-squares refinement [47] on F^2 was indicated by the maximum shift/error for the last cycle. The highest peaks in the final difference Fourier map were in the vicinity of the triflate oxygen atoms; the final map had no other significant features. A final analysis of variance between observed and calculated structure factors showed no dependence on amplitude or resolution. Atomic coordinates have been deposited with the Director of the Cambridge Crystallographic Data Center.

Acknowledgments—This research was supported by the U.S. Department of Energy through DEFG02-90-ER14146. We thank Atul Verma for advice on the crystallographic analysis.

REFERENCES

1. Topsøe, H., Clausen, B. S. and Massoth, F. E., *Hydrotreating Catalysis. Science and Technology*. Springer, Berlin (1996).
2. (a) Drew, L. J., In *Kirk-Othmer Encyclopedia of*

Chemical Technology (Edited by M. Howe-Grant) Vol. 18, p. 469. John Wiley & Sons, New York (1996); (b) Energy Information Administration *U.S. Crude Oil, Natural Gas, and Natural Gas Liquids Reserves*, p. 129. U.S. Department of Energy, Washington, DC (1991).
3. *Hydrocarbon Processing* 1996, **75,** 23.
4. Gates, B., *Catalytic Chemistry*. John Wiley, New York (1992).
5. Williamson, M., *Oil Gas J.* 1995, **93,** 47.
6. Ball, J. S., Wenger, W. J., Hyden, H. J., Horr C. A. and Myers, A. T., *ACS Petrol. Chem. Div. Preprints* 1956, **1,** 241.
7. Yen, T. F., *The Role of Trace Metals in Petroleum*. Ann Arbor Science, Ann Arbor, MI (1975).
8. (a) Triebs, A., *Liebigs Ann. Chem.* 1934, **509,** 103; (b) Triebs, A., *Liebigs Ann. Chem.* 1934, **510,** 42.
9. Treibs, A., *Liebigs Ann. Chem.* 1935, **517,** 172.
10. Baker, E. W., Corwin, A. H., Klesper, E. and Wei, P. E., *J. Org. Chem.* 1968, **33,** 3144.
11. (a) Pettersen, R. C. and Alexander, L. E., *J. Am. Chem. Soc.* 1968, **90,** 3873; (b) Petterson, R. C., *Acta Crystallogr., Sect. B* 1969, **25,** 2527.
12. Treibs, A., *Angew. Chem.*, 1936, **49,** 682.
13. *McGraw-Hill Dictionary of Scientific and Technical Terms* (Edited by D. N. Lapedes) McGraw-Hill, New York (1978).
14. Glebovskaia, E. A. and Vol'kenshtein, M. V., *Zh. Obshch. Khim.* 1948, **18,** 1440.
15. Falk, J. E., *Porphyrins and Metalloporphyrins*. Elsevier, New York (1964).
16. Phillips, J. N., *Res. Pure Appl. Chem.* 1960, **10,** 35.
17. Mitchell, P. C. H. and Scott, C. E., *Polyhedron* 1986, **5,** 237.
18. Rankel, L. A., *ACS Div. Petrol. Chem., Preprints* 1981, **26,** 689.
19. Hung, C. W. and Wei, J., *Ind. Eng. Chem. Process Des. Dev.* 1980, **19,** 250.
20. Chen, H. J. and Massoth, F. E., *Ind. Eng. Chem. Res.* 1988, **27,** 1629.
21. (a) Bonné, R. L. C., van Steenderen, P., van Diepen, A. E. and Moulijn, J. A., *Appl. Catal. A: Gen.* 1994, **108,** 171; (b) Ware, R. A. and Wei, J., *J. Catal.* 1985, **93,** 100.
22. Dailey, K. K., Yap, G. P. A., Rheingold, A. L. and Rauchfuss, T. B., *Angew. Chem. Int. Ed. Engl.* 1996, **35,** 1833. *Angew. Chem.* 1996, **108,** 1985. For a discussion of these results, see Senge, M. O., *Angew. Chem. Int. Ed. Engl.* 1996, **35,** 1923. *Angew. Chem.* 1996, **108,** 2051.
23. Dolphin, D. and Wick, A., *Tabulation of Infrared Spectral Data*, p. 469. Wiley, New York (1977).
24. Johnston, D. H., Gaswick, D. C., Lonergan, M. C., Stern, C. L. and Shriver, D. F., *Inorg. Chem.* 1992, **31,** 1869.
25. Structural studies on related Zn porphyrinates: Song, H., Orosz, R. D., Reed, C. A. and Scheidt, W. R., *Inorg. Chem.* 1990, **29,** 4274; Barkigia, K. M., Berber, M. D. Fajer, J. Medforth, C. J. Renner, M. W. and Smith, K. M., *J. Am. Chem. Soc.* 1990, **112,** 8850.
26. Cullen, D. L. and Meyer, E. F. Jr, *Acta. Cryst. B* 1976, **32,** 2259.
27. Brennan, T. D. and Scheidt, W. R., *Acta. Cryst. C* 1988, **44,** 478.
28. (a) Kuhn, N., *Bull. Soc. Chem. Belg.* 1990, **99,** 707; (b) Zakrzewski, J., *Heterocycles* 1990, **31,** 383; (c) Kerschner, D. L. and Basolo, F., *Coord. Chem. Rev.* 1987, **78,** 279.
29. (a) Fish, R. H., Baralt, E. and Kim, H. S., *Organometallics* 1991, **10,** 1965; (b) Kuhn, N., Horn, E.-M., Boese, R. and Augart, N., *Angew. Chem. Int. Ed. Engl.* 1989, **28,** 342; *Angew. Chem.* 1989, **101,** 354; (c) Felkin, H. and Zakrzewski, J., *J. Am. Chem. Soc.* 1985, **107,** 3374; (d) Öfele, K. and Dotzauer, E., *J. Organomet. Chem.* 1971, **30,** 211.
30. Joshi, K. K., Pauson, P. L. Qazi, A. R. and Stubbs, W. H., *J. Organomet. Chem.* 1964, **1,** 471; (b) Kelly, W. J. and Parthun, W. E., *Organometallics* 1992, **11,** 4348; (c) Kuhn, N., Köckerling, M., Stubenrauch, S., Bläser, D. and Boese, R., *J. Chem. Soc., Chem. Commun.* 1991, 1368; (d) Chase, K. J., Bryan, R. F., Woode, M. K. and Grimes, R. N., *Organometallics* 1991, **10,** 2631; (e) Kuhn, N., Kuhn, A. and Lampe, A. E. M., *Chem. Ber.* 1991, **124,** 997.
31. (a) Myers, W. H., Koontz, J. I. and Harman, W. D., *J. Am. Chem. Soc.* 1992, **114,** 5684; (b) Myers, W. H., Sabat, M. and Harman, W. D., *J. Am. Chem. Soc.* 1991, **113,** 6682; (c) Cordone, R. Harman, W. D. and Taube, H., *J. Am. Chem. Soc.* 1989, **111,** 5969.
32. Glueck, D. S., Hollander, F. J. and Bergman, R. G., *J. Am. Chem. Soc.* 1989, **111,** 2719.
33. (a) Pyshnograeva, N. I., Setkina, V. N., Andrianov, V. G., Struchkov, Y. T. and Kursanov, D. N., *J. Organomet. Chem.* 1980, **186,** 331; Pyshnograeva, N. I., Setkina, V. N., Andrianov, V. G., Struchkov Y. T. and Kursanov, D. N., *J. Organomet. Chem.* 1978, **157,** 431; (b) Pyshnograeva, N. I., Batsanov, A. S., Struchkov, Y. T., Ginsberg, A. G. and Setkina, V. N., *J. Organomet. Chem.* 1985, **297,** 69; (c) Reagen, W. K. and Radonovich, L. J. *J. Am. Chem. Soc.* 1989, **111,** 3881; 1987, **109,** 2193; (d) Kuhn, N., Horn, E.-M., Boese, R. and Bläser, D., *Chem. Ber.* 1989, **122,** 2275; (e) Floriani, C., *J. Chem. Soc., Chem. Commun.* 1996, 1257.
34. Lavallee, D. K., *The Chemistry and Biochemistry of N-Substituted Porphyrins*. VCH, New York (1987).
35. Zn(MeTPP)Cl: Lavallee, D. K., Kopelove, A. B. and Anderson, O. P., *J. Am. Chem. Soc.* 1978, **100,** 3025.
36. Co(MeTPP)Cl: Lavallee, D. K. and Anderson, O. P., *J. Am. Chem. Soc.* 1976, **98,** 4670.
37. Lavallee, D. K. and Anderson, O. P., *Inorg. Chem.* 1977, **16,** 1634.
38. DeMatteis, F. and Gibbs, A. H., *Biochem. J.* 1980, **187,** 285.
39. Gouterman, M., In *The Porphyrins* (Edited by D. Dolphin) Vol. 3, Chap. 1. Academic Press, New York (1978).
40. Bhyrappa, P. and Krishnan, V., *Inorg. Chem.* 1991, **30,** 239.
41. Bennett, M. A., Huang, T. N., Matheson, T. W. and Smith, A. K., *Inorg. Synth.* 1982, **21,** 74.

42. White, C. A., Yates and Maitlis, P. M., *Inorg. Synth.* 1992, **29,** 228.
43. Adler, A. D., Longo, F. R., Kampas, F. and Kim, J., *J. Inorg. Nucl. Chem.* 1970, **32,** 2443.
44. Siemens Industrial Automation, Incorporated, Madison, Wisconsin, U.S.A.
45. Wilson, A. J. C., ed. *International Tables for X-ray Crystallography* Vol. C. Kluwer Academic Publishers, Dordrecht (1992): (a) scattering factors, pp. 500–502; (b) anomalous dispersion corrections, pp. 219–222.
46. Sheldrick, G. M., *Acta Cryst.* 1990, **A46,** 467.
47. Sheldrick, G. M., SHELXL-93 (1993).